

Investigating the Post-Sintering Thermal and Mechanical Treatments on the Properties of Alumina Reinforced Aluminum Nanocomposites

Tayyab SUBHANI*, Abdulaziz S. ALGHAMDI, Abdul KHALIQ, Adnan MUNIR, Muhammad JAVAID IQBAL

Abstract: Alumina nanoparticles in the loading fraction of 3 wt% were incorporated in pure aluminum matrix to prepare nanocomposites for improved mechanical performance. Powder metallurgy route was adopted wherein nanoparticles were mixed with aluminium powder using dry mixing technique involving milling process, which was followed by the densification of composite mixture by uniaxial cold pressing and pressureless sintering. In order to increase the densification of nanocomposites, a batch of sintered nanocomposites was twice sintered at the same sintering parameters while another batch of specimens was cold pressed after initial sintering. The consolidated nanocomposites together with reference pure aluminum specimens were characterized microstructurally and mechanically by optical and electron microscopy, hardness and compressive strength tests. It was found that the hardness and compressive strength of nanocomposites after sintering increased up to ~ 29% and ~ 144% in comparison to pure aluminium specimens, respectively. Although the densification of nanocomposites increased after twice sintering, the hardness and compressive strength values decreased. However, the rise in consolidation along with improved mechanical performance was noted after cold pressing the specimens as secondary treatment after sintering; hardness increased up to ~ 36% while compressive strength rose to ~ 64%. In comparison to twice sintering, cold pressing after initial sintering significantly increased the hardness and compressive strength of nanocomposites up to ~ 76% and ~ 301% with reference to pure aluminum, respectively. It was found that both the incorporation of alumina nanoparticles and cold pressing after initial sintering improved the mechanical properties of nanocomposites.

Keywords: alumina; hardness; nanocomposite; powder metallurgy; sintering

1 INTRODUCTION

Metal matrix composites (MMCs) constitute a prominent class of composite materials incorporating oxides, nitrides, carbides, borides and the allotropes of carbon in metallic matrices typically aluminum, magnesium, titanium, copper and their alloys [1]. Among different metallic matrices, aluminum is considered as the most investigated matrix material due to its low density, corrosion resistance, recyclability and especially the ability to increase the strength-to-weight, thus making the aluminum matrix composites (AMCs) an attractive choice for aerospace and automotive industries [2]. In AMCs, high strength and stiffness are derived from thermodynamically stable ceramic reinforcements while ductility and toughness arrive from metallic matrices [3].

Among a variety of AMCs, particulate reinforced composites have earned a significant importance in composite science and technology due to their near-isometric mechanical and functional performance, high-temperature stability and improved toughness [4] and tribological properties [5]. A range of reinforcements are incorporated in pure aluminum and its alloys including Al_2O_3 , Y_2O_3 , Si_3N_4 , AlN , TiC , SiC , TiB_2 and B_4C [6]. Iron oxide is still another reinforcement used in aluminum matrices. Among different particulate reinforcements, alumina (Al_2O_3) is the one most commonly used, which improves the mechanical attributes of the developed composites containing aluminum as matrix [7].

After the emergence of nanotechnology, the field of composites acquired a novel concept of incorporating nanoreinforcements, thus developing a new class of composites named as nanocomposites [8]. The essential requirement of the nanoreinforcements in nanocomposites is their size, i.e. ≤ 100 nm, which may be their diameter as in case of nanoparticles, nanotubes or nanofibers or thickness as in nanosheets or nanoplatelets [9]. In this respect, the incorporation of alumina nanoparticles developed the next generation of alumina reinforced aluminum matrix composites, which captured immediate

attention for further improvement in properties of traditional AMCs [10].

The liquid [11] and solid state [12] processing routes are common for the fabrication of AMCs containing alumina nanoparticles together with the in situ formation [13]. Liquid state processing includes stir casting, ultrasonic dispersion, disintegrated melt dispersion, and selective laser melting [14]. One of the solid state processes is based upon powder metallurgy technique and comprises two steps: (a) preparation of composite mixture followed by its (b) consolidation [15]. The composite mixture is usually produced by conventional mixing, mechanical alloying or high energy ball milling while consolidation of the composite mixture is performed by pressureless or pressure-assisted sintering techniques including cold/hot pressing, cold/hot isostatic pressing or other techniques such as equal channel angular pressing [16]. In order to further increase the properties of composites developed by liquid or solid state processing, a secondary treatment is applied, which may be thermal, mechanical or thermo-mechanical. The common secondary processes include rolling, forging or extrusion both in cold or hot conditions, and heat-treatment [17].

The strengthening mechanisms in AMCs include the load-transfer effect, Hall-Petch strengthening (grain boundary strengthening), coefficient of thermal expansion and elastic modulus mismatch, and Orowan strengthening [18]. The strengthening due to load-transfer is because of the high strength and hardness of reinforcement while the grain size refinement is responsible for Hall-Petch strengthening. Coefficient of thermal expansion and elastic modulus mismatch create dislocations around the particles while Orowan strengthening emerges due to the interaction of nanoparticles with dislocations [19]. Owing to the metallic matrix, the AMCs enjoy other strengthening mechanisms usually activated in metals and alloys such as work hardening, solid-solution strengthening, and precipitation hardening [20].

Generally, the developed composites are utilized in as

developed state and offer promising mechanical property improvements [21]. However, the application of a secondary process further increases the mechanical performance of composites. Recently, alumina-aluminum composite system has been developed by stir casting process and a secondary process of rolling was incorporated to improve the properties [22]. In a different investigation, hot-extrusion was applied after processing the composite by cold-press sintering [23].

In the present study, nanocomposites were prepared by adding 3 wt% nanoparticles of alumina in a pure aluminum matrix to investigate their effects on the properties such as hardness and compressive strength and modification in densification after twice sintering and coldpressing after initial sintering. The aim was to investigate the effect of secondary processes, i.e. thermal and mechanical treatments upon the microstructural evolution and mechanical property improvement.

2 EXPERIMENTAL

2.1 Materials

99.5% pure aluminum powder of diameter $\sim 6 - 10 \mu\text{m}$, as produced by gas atomization was used as the matrix material in the present work. The spherical morphology of the aluminum power with attached satellite particles is shown in Fig. 1a. Alumina nanoparticles of particle size $\sim 50 \text{ nm}$ was used as the reinforcement, as shown in Fig. 1b. Aluminum powder and alumina nanoparticles were procured from Merck, Germany and Metkon Technology, respectively.

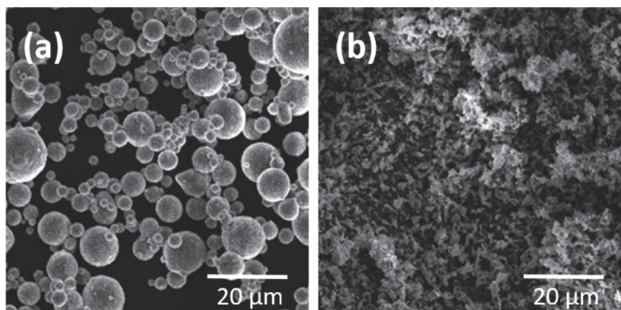


Figure 1 (a) Pure aluminum powder and (b) alumina nanoparticles used in the present study for preparing nanocomposites

2.2 Manufacturing

For the preparation of nanocomposite specimens, 3 wt% alumina nanoparticles were dry mixed in 97 wt% aluminum powder. The composite mixture was sealed in a stainless steel vessel of diameter 25 mm and height 70 mm and milled in a high-capacity laboratory milling machine (RZ-04149-05, Cole-Parmer, USA) at 300 rpm for 3 h at room temperature. Zirconia balls with diameter 5 mm and weight 5 g were used as milling media and ball-to-powder ratio was kept at 10:1. After the milling process, the composite mixture was kept in a sealed vial to avoid the inclusion of moisture or contamination. The reference pure aluminum specimens were also milled using the same milling parameters so that these could bear the same mechanical working effect induced by the milling operation.

The consolidation of composite powders was

performed after milling process. The composite mixture in required quantity was filled in a steel die of internal diameter 10 mm and subsequently consolidated under a hydraulic press (Specac Hydraulic Press, Specac Limited, United Kingdom). Prior to filling, the inner surface of the steel die was washed with ethanol while the applied pressure for pressing the specimens was 125 MPa. After cold compaction of the composite powder, the green bodies in cylindrical shapes were carefully removed from the steel die and sintered in a box-type resistance furnace (Thermolyne, Thermo Scientific). The sintering cycle comprised the heating rate of 5 °C/min up to 630 °C and holding at that temperature for 3 h, followed by furnace cooling. The same process was repeated for the preparation of pure aluminum specimens for the purpose of comparison with nanocomposite specimens.

A planned experimental research was performed. A total of three batches of specimens were prepared, each comprising (a) nanocomposites containing 3 wt% alumina nanoparticles and (b) reference pure aluminum specimens. The first batch was characterized in as-sintered condition, while the second batch was sintered again at the same sintering parameters as adopted for the initial sintering process. The third batch of specimens was cold pressed after initial sintering. The prepared composite and reference pellets were subsequently characterized for microstructural, physical and mechanical properties. The schematic of the complete nanocomposite preparation process is depicted in Fig. 2 and the details of the specimens are given in Tab. 1.

2.3 Characterization

The density values of green and sintered specimens were measured by buoyancy method (Archimedes principle). A densimeter was used with an accuracy of 10^{-3} g (AU-900S, DongGuan HongTuo Instrument Company, China).

In order to observe the microstructure of the specimens, these were examined under optical microscope (IMM-901, Metkon Instruments, Turkey) and scanning electron microscope (MIRA-III, FEG-SEM, Tescon Orsay Holding, Brno, Czech Republic). Optical micrographs were acquired up to a magnification of 200 \times . SEM images were captured in the secondary electron imaging mode at an accelerating voltage of 10 kV. The composite specimens were attached on the aluminum stubs with carbon tape; polished specimens were observed under SEM.

To obtain polished surfaces for hardness, compressive test and microscopy, the specimens were ground with SiC emery papers of grit size 320, 800, 1200, 1600, which was followed by polishing. Pure aluminum specimens were polished using alumina powder of size 1.0 μm while composite specimens were polished using diamond suspension of the same size. After the polishing process, the etching of the specimens was performed with Keller's reagent (5 mL HNO₃, 2 mL HF, 3 mL HCl, and 190 mL distilled water) with an immersion time of 30 s. ASTM B821-10 and ASTM E407 standards were followed to prepare and etch metallurgical specimens.

The hardness of the prepared specimens was measured using Vickers microhardness testing machine (VLS 3853, Shimadzu, Japan). The hardness testing was performed at

the indenter load of 100 g for the dwell time of 5 s. At least five values of each specimen were acquired to obtain an average value. ASTM E92-16 standard was followed to test the Vickers hardness of specimens. It is to be noted that the hardness test was performed on the surface of the specimens parallel to the applied uniaxial load during cold

pressing. For compression testing, a universal testing machine (WDW-30, Jinan Testing Equipment IE Corporation, China) was employed at a strain rate of 0.2 mm/min. At least five tests of each specimen were performed while the size of the specimens was diameter 8 mm and thickness 4 mm.

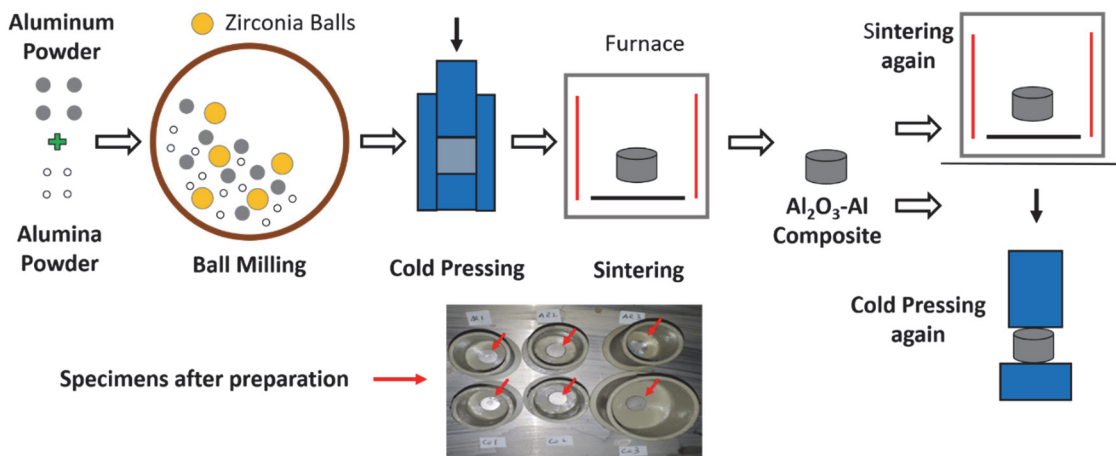


Figure 2 Schematic of pure aluminum and nanocomposite preparation process used in the present study

Table 1 Pure aluminum and nanocomposite specimens prepared in the present study

Specimens	As-sintered	Twice Sintering	Cold pressed after sintering
Pure Aluminum	100 wt% Al	100 wt% Al	100 wt% Al
Nanocomposite	3 wt% Al ₂ O ₃ + 97 wt% Al	3 wt% Al ₂ O ₃ + 97 wt% Al	3 wt% Al ₂ O ₃ + 97 wt% Al

Table 2 Relative densities of pure aluminum and nanocomposite specimens after sintering, twice sintering and cold pressing after sintering

Specimens	Green Density / %	As-sintered / %	Twice Sintering / %	Cold Pressed after Sintering / %
Pure Al-01	60.1 ± 1.4	96.3 ± 1.5	-	-
Pure Al-02	60.3 ± 1.7	95.9 ± 1.3	97.9 ± 1.6	-
Pure Al-03	59.9 ± 1.2	96.1 ± 1.1	-	99.4 ± 1.5
Nanocomposite-01	59.8 ± 1.1	94.9 ± 1.3	-	-
Nanocomposite-02	60.1 ± 1.6	95.1 ± 1.4	97.1 ± 1.3	-
Nanocomposite-03	59.9 ± 1.5	94.7 ± 1.9	-	98.9 ± 1.9

3 RESULTS AND DISCUSSION

3.1 Density

Tab. 2 shows the relative green and sintered densities of the reference and nanocomposite specimens; the densities of the specimens after sintering twice and cold pressing after initial sintering are also presented. The relative densities were calculated after measuring the actual densities from buoyancy method and calculating the theoretical densities from the rule of mixtures. The densities of aluminum and alumina were taken to be 2.7 g/cm³ and 3.95 g/cm³ for calculating the theoretical densities of nanocomposites, respectively. Being heavier than aluminum, the addition of alumina in aluminum is expected to increase the density of nanocomposites. However, the addition of 3 wt% alumina nanoparticles increases the density of nanocomposites from 2.70 g/cm³ to 2.74 g/cm³ yielding a rise of only 1.4%.

Fig. 3 shows the graphical presentation of the densities of three batches of reference pure aluminum (Fig. 3a) and nanocomposites (Fig. 3b). It can be seen that the green densities of all specimens are ~ 60% while the sintered specimens have densities approaching ~ 95%. Further rises in the densities were observed after the application of thermal and mechanical secondary processes, i.e. twice sintering and cold pressing after initial sintering, which enhanced the densities to > 97% and > 99%, respectively.

It is to be noted that the achievement of ~ 60% green densities indicates acceptable values provided the incorporation of alumina nanoparticles, and compares with the literature values [24]. The achievement of ~ 95% sintered densities is also promising while considering the fact that pressureless sintering technique was employed while in case of pressure-assisted methods, the values could be increased further. Indeed the densities of the prepared nanocomposites ~ 99% match with published data [25] and provide the opportunity to explore the reinforcing effect of alumina nanoparticles especially in mechanical performance, as discussed further below.

It was also observed that the densities of the nanocomposites were comparatively lesser than pure aluminum specimens, which is in good agreement with the available data in literature [26]; composites offer less densities due to their heterogeneity in composition in comparison to pure metals or alloys, which arrives due to the incorporation of reinforcement in matrix material. The effect of mechanical working in the form of cold pressing was significant (98.9 ± 1.9%) to increase the densities of specimens than thermal treatment, i.e. twice sintering (97.1 ± 1.3%) for nanocomposites, which indicates a comparative rise of ~ 2%. It can also be expected that the simultaneous application of pressure with heat may provide a practical density of nanocomposites equivalent to theoretical density.

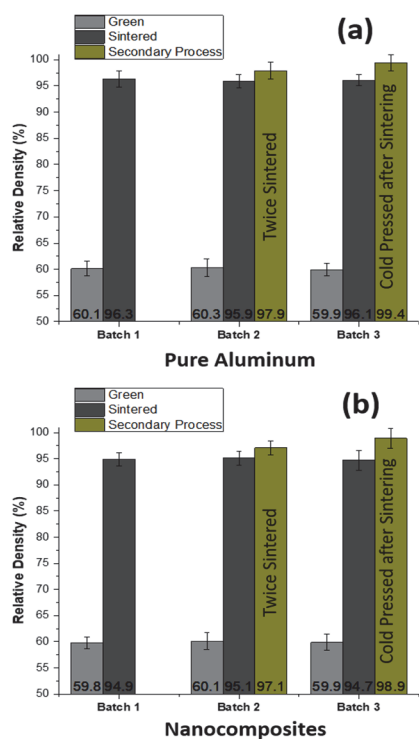


Figure 3 Relative densities of pure aluminum (a) and nanocomposites (b) in green state, after sintering and after secondary process: twice sintering and cold pressing after sintering

3.2 Microstructural Evolution

The microstructures of pure aluminum and nanocomposite specimens after sintering, twice sintering and cold pressing after sintering are shown in Fig. 4. The digital imaging contrast was kept constant for capturing all images. It can be noted that the images show the densification of specimens corresponding to their measured densities, as discussed above. The porosity level in the as-sintered specimens matches with their density (~ 95%) while improved densification (~ 97%) can be witnessed in specimens after twice sintering. The specimens which were cold pressed after initial sintering revealed the densification up to ~ 99%. Likewise, the images in the three batches show gradual decrease in the porosity level. Due to nanometer size of alumina, it is impossible to identify their presence at the chosen magnification under light microscopy. The bonding of the aluminum particles is also visible after sintering. The images of 3 wt% Al_2O_3 -Al nanocomposites which were cold pressed after sintering were acquired at two magnifications under SEM to observe the quality of densification, as shown in Fig. 5. The images indicate the absence of porosity and any other defects while the detection of alumina nanoparticles due to their nanometer size is still difficult to detect at these magnifications. Nevertheless, the presence of the clusters of alumina nanoparticles or any other defects is absent. A similar observation of optical microstructures was made after incorporating CNTs and ZrB_2 particles in aluminum powder [6].

3.3 Grain Size

Using the optical micrographs of the composite specimens, the grain size was measured, as plotted in

Fig. 6. The particle size of as-received aluminum powder was ~ 10 μm while the grain sizes of pure aluminum and nanocomposite specimens after sintering were found to be $13.4 \pm 2.1 \mu\text{m}$ and $12.1 \pm 1.9 \mu\text{m}$, respectively. The increase in diameter may be due to sintering process or prior uniaxial cold pressing in steel die during the formation of green bodies. As the soft aluminum particles were compressed vertically under pressure, their size increased horizontally. The grain sizes of pure aluminum and nanocomposites increased to $19.7 \pm 3.4 \mu\text{m}$ and $17.8 \pm 4.1 \mu\text{m}$ after twice sintering thus showing the rises of ~ 44% and ~ 47%, respectively; the thermal treatment of the specimens during twice sintering is solely responsible for the increase in the grain size, which adversely affects the hardness, as discussed further below.

However, it is worth noting that the grain size of nanocomposites is comparatively smaller than pure aluminum specimens in sintered, twice sintered and cold pressed after sintering specimens. One of the possible reasons may be the incorporation of alumina nanoparticles, which impeded the grain growth during heating. During the milling process prior to sintering, the alumina nanoparticles were imbedded on the surface of soft aluminum particles, which may have caused hindrance during grain growth.

The specimens which were cold pressed after sintering showed the maximum values of grain sizes, i.e. $35.4 \pm 4.5 \mu\text{m}$ and $32.1 \pm 4.1 \mu\text{m}$ for pure aluminum and nanocomposites showing the rises of ~ 164% and ~ 165%, respectively. It is due to the reason that the grains were flattened when coldpressed uniaxially and these values actually give the diameter with very low thickness of individually sintered aluminum particles. Nevertheless, due to cold working (strain hardening), the hardness of the specimens is expected to increase significantly, as discussed further below.

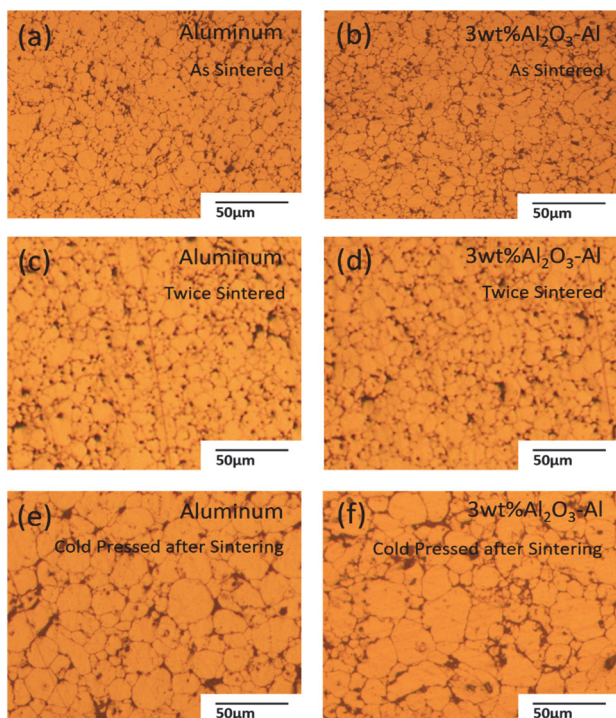


Figure 4 Optical micrographs of pure aluminum (a, c, e) and nanocomposites (b, d, f) after sintering (a, b), twice sintering (c, d), and cold pressing after sintering (e, f)

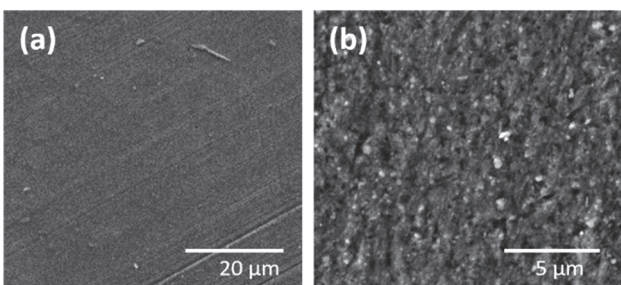


Figure 5 SEM images of 3 wt% Al_2O_3 -Al nanocomposites cold pressed after sintering at two different magnifications: (a) polished and (b) as fracture surfaces

3.4 Hardness

Fig. 7 shows the hardness values of pure aluminum and nanocomposite specimens. Pure aluminum showed a hardness value of 25.4 ± 2.7 HV while the nanocomposites revealed the value of 32.8 ± 2.9 HV. It can be observed that after adding 3 wt% alumina nanoparticles, the hardness of nanocomposite specimens increased up to $\sim 29\%$ in comparison to pure aluminum specimens after initial sintering. However, after twice sintering, the hardness values of both the pure aluminum and nanocomposites decreased to 24.1 ± 2.5 HV and 27.3 ± 1.9 HV; the value of pure aluminum decreased to $\sim 5\%$ while nanocomposite value lowered to $\sim 17\%$. Nevertheless, after twice sintering, the value of nanocomposites (27.3 ± 1.9 HV) is still higher than pure aluminum sintered for one time (25.4 ± 2.7 HV). It is surprising to note that after twice sintering, the hardness values of nanocomposites decreased despite the fact that the sintered density increased. The decrease in hardness after twice sintering may be related to increase in the grain size or it may be due to the stress relieving process after twice sintering.

In comparison, the hardness values increased after cold pressing the specimens after initial sintering; the rises of $\sim 57\%$ and $\sim 36\%$ were observed for pure aluminum (39.8 ± 3.4 HV) and nanocomposites (44.7 ± 4.1 HV) in comparison to sintered specimens, respectively. Both the increase in the densification of specimens and the strain hardening due to cold pressing appear to be the possible reasons of the rises in hardness values. In comparison to pure aluminum sintered for one time (25.4 ± 2.7 HV), the nanocomposites cold pressed after sintering revealed the hardness value of 44.7 ± 4.1 HV showing a significant rise of $\sim 76\%$.

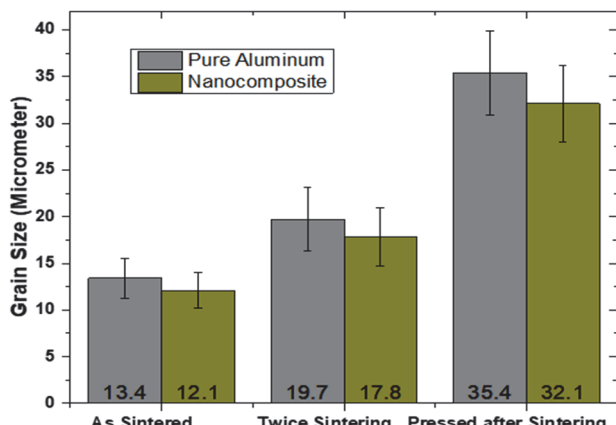


Figure 6 Grain size of pure aluminum and nanocomposites measured after sintering, twice sintering and cold pressing after sintering

In a different study, $\sim 7\%$ hardness was increased after incorporating 0.5 wt% CNTs in aluminum matrix, while 22% improvement in hardness was noticed after adding 5 wt% ZrB_2 particles [6]. The present study showed an improvement of $\sim 29\%$ after incorporating 3 wt% alumina nanoparticles, which is attributed to the nanometer size of alumina particles.

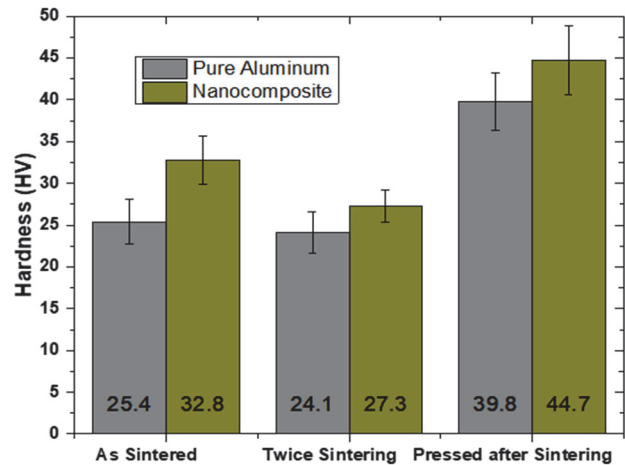


Figure 7 Hardness values of pure aluminum and nanocomposites after sintering, twice sintering and cold pressing after sintering

3.5 Compressive Strength

Fig. 8 plots the compressive strength values of pure aluminum and nanocomposite specimens. Pure aluminum showed a strength value of 15.5 ± 1.9 MPa while the nanocomposites revealed the value of 37.8 ± 2.6 MPa. It can be observed that after adding 3 wt% alumina particles, the compressive strength of the nanocomposite specimens increased up to $\sim 144\%$ in comparison to pure aluminum specimens after initial sintering. However, after twice sintering, the compressive strength values of both the pure aluminum and nanocomposite specimens decreased to 9.7 ± 1.1 MPa and 21.4 ± 1.7 MPa, respectively; the value of pure aluminum decreased to $\sim 37\%$ while nanocomposite value lowered to $\sim 43\%$. Nevertheless, after twice sintering, the value of nanocomposites (21.4 ± 1.7 MPa) is still higher than pure aluminum sintered for one time (15.5 ± 1.9 MPa).

In comparison, the compressive strength values increased after cold pressing the specimens after initial sintering; the rises of $\sim 170\%$ and $\sim 64\%$ were observed for pure aluminum (41.9 ± 3.1 MPa) and nanocomposites (62.3 ± 4.5 MPa) in comparison to sintered specimens. Both the increase in the densification of specimens and the strain hardening due to cold-pressing appears to be the possible reasons of the rises in compressive strength values. In comparison to pure aluminum sintered for one time (15.5 ± 1.9 MPa), the nanocomposites cold pressed after sintering revealed the compressive strength value of (62.3 ± 4.5 MPa) showing a significant rise of $\sim 301\%$. The compressive strength results complement the hardness values, as the hardness of pure aluminum and nanocomposites decreased after twice sintering and increased after cold pressing followed by initial sintering.

In a separate study, an improvement of $\sim 117\%$ in hardness was observed after adding 6 wt% B_4C particles [7] while in a different study, an improvement in hardness

of ~ 27 % was found after incorporating 5 wt% ZrB₂ particles [6], while the present research offers a significant rise of ~ 144 % owing to the nanometer size of alumina particles.

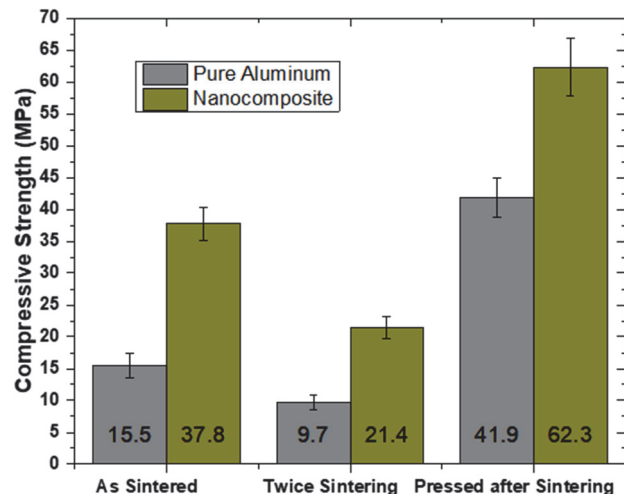


Figure 8 Compressive strength of pure aluminum and nanocomposites after sintering, twice sintering and cold pressing after sintering

4 CONCLUSIONS

Aluminum matrix nanocomposites were successfully manufactured by incorporating nanoparticles of alumina in pure aluminum matrix for improved mechanical properties. Alumina nanoparticles in the loading fraction of 3 wt% were added to fabricate nanocomposites along with reference specimens of pure aluminum. Powder metallurgy route was chosen wherein nanoparticles were mixed with aluminium powder using dry mixing technique and milling process. The densification of specimens was achieved by uniaxial cold pressing followed by pressureless sintering while improved densification was achieved by twice sintering and cold pressing after sintering. The following conclusions are drawn:

- The incorporation of 3 wt% alumina particles in pure aluminium matrix increased the hardness and compressive strength of nanocomposites up to ~ 29% and ~ 144%, respectively.
- The twice sintering increased the densification by ~ 2% but it decreased the hardness and compressive strength down to ~ 17% and ~ 43%, respectively.
- The cold pressing after initial sintering increased the densification by ~ 4% and it further increased the hardness and compressive strength of nanocomposites up to ~ 36% and ~ 64%, respectively.
- In comparison to twice sintering, the application of secondary process in the form of cold pressing after initial sintering significantly increased the hardness and compressive strength of nanocomposites up to ~ 76% and ~ 301% with reference to pure aluminum, respectively.
- The developed nanocomposites are potential candidate materials for structural applications in aerospace and automotive industries demanding improved mechanical performance.

Acknowledgements

This research has been funded by Scientific Research Deanship at the University of Ha'il, Saudi Arabia through project number RG-21 065.

5 REFERENCES

- Lakshminthan, A., Angadi, S., Malik, V., Saxena, K. K., Prakash, C., Dixit, S., & Mohammed, K. A. (2022). Mechanical and Tribological Properties of Aluminum-Based Metal-Matrix Composites. *Materials*. <https://doi.org/10.3390/ma15176111>
- Khan, M., Rehman, A., Aziz, T., Shahzad, M., Naveed, K., & Subhani, T. (2018). Effect of inter-cavity spacing in friction stir processed Al 5083 composites containing carbon nanotubes and boron carbide particles. *Journal of Materials Processing Technology*, 253. <https://doi.org/10.1016/j.jmatprotec.2017.11.002>
- Khan, M., Rehman, A., Aziz, T., Naveed, K., Ahmad, I., & Subhani, T. (2017). Cold formability of friction stir processed aluminum composites containing carbon nanotubes and boron carbide particles. *Materials Science and Engineering A*, 696. <https://doi.org/10.1016/j.msea.2017.04.074>
- Prince, M., Vinodh Kumar, A., Mohan Kumar, G. (2022). Investigation on Mechanical Properties of Aluminum 8011 Metal Matrix Composite with Titanium Carbide Particulate Reinforcement. *Technical Gazette*, 29(6), 2105-2110. <https://doi.org/10.17559/TV-20220217173159>
- Deshmukh, S., Joshi, G., Ingle, A., & Thakur, D. (2021). An overview of Aluminium Matrix Composites: Particulate reinforcements, manufacturing, modelling and machining. *Materials Today: Proceedings*, 46, 8410-8416. <https://doi.org/https://doi.org/10.1016/j.matpr.2021.03.450>
- Farooqi, A., Ahmed, M., Subhani, T., & Husain, S. W. (2019). Hybrid aluminum matrix composites containing carbon nanotubes and zirconium diboride particles: fractography, microstructure and mechanical performance. *SN Applied Sciences*, 1(12). <https://doi.org/10.1007/s42452-019-1767-7>
- Khan, M., Zulfaqar, M., Ali, F., & Subhani, T. (2017). Hybrid aluminium matrix composites containing boron carbide and quasicrystals: manufacturing and characterisation. *Materials Science and Technology (United Kingdom)*, 33(16). <https://doi.org/10.1080/02670836.2017.1342017>
- Khan, M., Zulfaqar, M., Ali, F., & Subhani, T. (2017). Microstructural and mechanical characterization of hybrid aluminum matrix composite containing boron carbide and Al-Cu-Fe quasicrystals. *Metals and Materials International*, 23(4). <https://doi.org/10.1007/s12540-017-6619-7>
- Wang, F., Liu, H., Liu, Z., Guo, Z., & Sun, F. (2022). Microstructure analysis, tribological correlation properties and strengthening mechanism of graphene reinforced aluminum matrix composites. *Scientific Reports*, 12(1), 9561. <https://doi.org/10.1038/s41598-022-13793-y>
- Poirier, D., Drew, R. A. L., Trudeau, M. L., & Gauvin, R. (2010). Fabrication and properties of mechanically milled alumina/aluminum nanocomposites. *Materials Science and Engineering: A*, 527(29), 7605-7614. <https://doi.org/https://doi.org/10.1016/j.msea.2010.08.018>
- Vijayan, S. N., Samson, J. S. C., Saiyath Ibrahim, A., Ramesh Babu, R., Prakash, P., & Gnanasekaran, S. (2022). A Review on Manufacturing of Aluminium Alloy Based Metal Matrix Composites through Stir Casting Route. *Functional Composite Materials: Manufacturing Technology and Experimental Application*, 56-70. <https://doi.org/10.2174/9789815039894122010007>

- [12] Chak, V., Chattopadhyay, H., & Dora, T. L. (2021). Application of solid processing routes for the synthesis of graphene-aluminum composites. *Materials and Manufacturing Processes*, 36(11), 1219-1235. <https://doi.org/10.1080/10426914.2021.1914845>
- [13] Anwar, J., Khan, M., Farooq, M. U., Khan, T. F., Anwar, G. A., Qadeer, A., & Subhani, T. (2022). Effect of B4C and CNTs' nanoparticle reinforcement on the mechanical and corrosion properties in rolled Al 5083 friction stir welds. *Canadian Metallurgical Quarterly*, 1-10. <https://doi.org/10.1080/00084433.2022.2054586>
- [14] Sharma, A. K., Bhandari, R., & Pinca-Bretorean, C. (2021). A systematic overview on fabrication aspects and methods of aluminum metal matrix composites. *Materials Today: Proceedings*, 45, 4133-4138. <https://doi.org/https://doi.org/10.1016/j.matpr.2020.11.899>
- [15] Leparoux, M., Kollo, L., Kwon, H., Kallip, K., Babu, N. K., AlOgab, K., & Talari, M. K. (2018). Solid State Processing of Aluminum Matrix Composites Reinforced with Nanoparticulate Materials. *Advanced Engineering Materials*, 20(11), 1800401. <https://doi.org/https://doi.org/10.1002/adem.201800401>
- [16] Ramu, G. & Bauri, R. (2009). Effect of equal channel angular pressing (ECAP) on microstructure and properties of Al-SiCp composites. *Materials & Design*, 30, 3554-3559. <https://doi.org/10.1016/j.matdes.2009.03.001>
- [17] Mazahery, A. & Shabani, M. O. (2014). The effect of primary and secondary processing on the abrasive wear properties of compocast aluminum 6061 alloy matrix composites. *Protection of Metals and Physical Chemistry of Surfaces*, 50(6), 817-824. <https://doi.org/10.1134/S2070205114060021>
- [18] Sharma, V., Prakash, U., & Kumar, B. V. M. (2015). Surface composites by friction stir processing. *Journal of Materials Processing Technology*, 224, 117-134. <https://doi.org/https://doi.org/10.1016/j.jmatprotec.2015.04.019>
- [19] Hao, S. & Xie, J. (2013). Tensile properties and strengthening mechanisms of SiCp-reinforced aluminum matrix composites as a function of relative particle size ratio. *Journal of Materials Research*, 28(15), 204-2055. <https://doi.org/10.1557/jmr.2013.202>
- [20] Hu, Z., Tong, G., Lin, D., Chen, C., Guo, H., Xu, J., & Zhou, L. (2016). Graphene-reinforced metal matrix nanocomposites. *Materials Science and Technology*, 32(9), 930-953. <https://doi.org/10.1080/02670836.2015.1104018>
- [21] Asghar, Z., Latif, M. A., Rafi-ud-Din, Nazar, Z., Ali, F., Basit, A., & Subhani, T. (2018). Effect of distribution of B \leq 4 \leq C on the mechanical behaviour of Al-6061/B \leq 4 \leq C composite. *Powder Metallurgy*, 61(4). <https://doi.org/10.1080/00325899.2018.1501890>
- [22] Gupta, A., Mallik, B., & Roy, D. (2020). Structure Property Correlation of In Situ Reinforced Al-based Metal Matrix Composite via Stir Casting. *Materials Performance and Characterization*, 9, 20190038. <https://doi.org/10.1520/MPC20190038>
- [23] Fang, Z., Zhao, Y., Kai, X., Tao, R., Xia, C., Zhang, Z., & Sun, Y. (2020). Hot deformation behavior of the AA6016 matrix composite reinforced with in situ ZrB₂ and Al₂O₃ nanoparticles. *Materials Research Express*, 7(2), 26508. <https://doi.org/10.1088/2053-1591/ab6e34>
- [24] Singh, N. P., Gupta, V. K., & Singh, A. P. (2019). Graphene and carbon nanotube reinforced epoxy nanocomposites. *Polymer*, 180, 121724. <https://doi.org/https://doi.org/10.1016/j.polymer.2019.121724>
- [25] Rashad, M., Pan, F., Tang, A., & Asif, M. (2014). Effect of Graphene Nanoplatelets addition on mechanical properties of pure aluminum using a semi-powder method. *Progress in Natural Science: Materials International*, 24(2), 101-108. <https://doi.org/https://doi.org/10.1016/j.pnsc.2014.03.012>
- [26] Ipekoglu, M., Nekouyan, A., Albayrak, O., & Altintas, S. (2017). Mechanical characterization of B4C reinforced aluminum matrix composites produced by squeeze casting. *Journal of Materials Research*, 32(3), 599-605. <https://doi.org/10.1557/jmr.2016.495>

Contact information:**Tayyab SUBHANI**

(Corresponding author)

College of Engineering, University of Ha'il,
Ha'il P.O. Box 2440, Saudi Arabia
E-mail: drtayyabsubhani@gmail.com**Abdulaziz Salem ALGHAMDI**College of Engineering, University of Ha'il,
Ha'il P.O. Box 2440, Saudi Arabia**Abdul KHALIQ**College of Engineering, University of Ha'il,
Ha'il P.O. Box 2440, Saudi Arabia**Adnan MUNIR**School of Mechanical and Manufacturing Engineering,
National University of Sciences and Technology,
Islamabad, Pakistan**Muhammad Javaid IQBAL**Centre of Excellence in Solid State Physics,
University of the Punjab,
Lahore 54590, Pakistan